Novel insights in MHC class II antigen presentation

Hoorn, B.M. van den

Chapter 2
Dynamics of proteins within tetraspanin webs in MVBs

(Submitted to Journal of Cell Science)

Dynamics of proteins within tetraspanin webs in MVBs

Tineke van den Hoorn, Lennert Janssen, Hans Janssen, and Jacques Neefjes*

Division of Cell Biology, The Netherlands Cancer Institute, Plesmanlaan 121,1066 CX Amsterdam NL
* Correspondence j.neefjes@nki.nl

Summary

Late endosomal multi-vesicular bodies are complicated organelles with various subdomains located at the limiting membrane (LM) and the internal vesicles (ILV). ILV accumulate tetraspanins, such as CD63 and CD82 that may form protein networks including associated proteins. Here, we studied the dynamics of tetraspanin networks made by CD63 and CD82 with two associated proteins; Major Histocompatibility Complex class II (MHC-II) and its chaperone HLA-DM (DM). Using confocal FRET technology, we measured energy transfer between different fluorescently tagged proteins within the MVB. We observed stable interactions for CD63-CD82 in the two subdomains but altered interactions between CD63 or CD82 pairs. The interactions between DM and MHC-II with the two tetraspanins also changed in the two MVB subdomains. This suggests that MHC-II and DM reposition in the tetraspanin networks in the two subdomains of a MVB. These data visualize for the first time protein dynamics in tetraspanin networks of MVB subdomains.

Introduction

MIICs are multivesicular bodies (MVB) or multilamellar structures of acidic pH, containing MHC-II and DM molecules, as well as proteases (Neefjes, 1999). Their architecture is unique; a limiting membrane (LM) surrounds a large set of small vesicles termed intraluminal vesicles (ILV) that are generated by the ESCRT machinery (Teis et al., 2009). This machinery selects ubiquitin-tagged proteins for sorting into ILV, resulting in a distinct composition of two subdomains of the same MVB, the ILV and the LM. Tetraspanins and other molecules such as lipids like Lyso-Bis-Phosphatidic Acid (LBPA) concentrate in ILV, whereas other proteins like LAMP are found predominantly on the LM (Griffiths et al., 1988). Major Histocompatibility Complex class II molecules (MHC-II) present antigenic peptide fragments, acquired in the endocytic route, to the immune system. In humans, three MHC-II alleles exist named Human Leukocyte Antigen (HLA)-DR, -DP and –DQ. MHC-II consists of $\alpha\beta$-heterodimers, which assemble in the ER with the invariant chain (Ii). Ii fills the peptide loading groove of MHC-II and targets MHC-II to late endosomal compartments, generally named MIIC (Neefjes et al., 1990; Peters et al., 1991; Roche and Cresswell, 1990). Here, Ii is degraded by resident proteases, except for a short fragment called CLIP that is protected by the surrounding peptide-binding groove. The chaperone DM also resides in MIIC

and facilitates the exchange of CLIP for high-affinity binding peptides generated by resident proteases (Denzin and Cresswell, 1995; Kropshofer et al., 1997). While MHC-II and DM are found both on the LM and ILV of the MVB, they interact predominantly in the ILV. Consequently, MHC-II peptide loading in phagosomes (which consist of LM only) fails (Zwart et al., 2005).
It is unclear why MHC-II fails to interact with DM at the LM of MIIC. One possibility is that tetraspanin proteins or networks concentrate these molecules and stabilize their interaction. The tetraspanins CD63 and CD82 are enriched in ILV (Escola et al., 1998) and form complexes with MHC-II (here HLA-DR), DM and HLA-DO molecules as detected by biochemical experiments (Engering and Pieters, 2001; Hammond et al., 1998), but the biological consequences of these interactions are unclear.
Tetraspanins probably form supramolecular complexes or microdomains, also called a tetraspanin-web (Rubinstein et al., 1996). Cryo-electron microscopy studies show that tetraspanins can assemble into highly regular protein complexes. Tetraspanins may organize other proteins into these supramolecular-webs to facilitate protein interactions (Min et al., 2006) and this may also explain why MHC-II interacts preferentially with DM on ILV (Zwart et al., 2005).
We hypothesized that tetraspanins on ILV act as a MHC-II peptide-loading platform by stabilizing interactions between MHC-II and DM. Consequently, the interaction between MHC-II and DM with tetraspanin constituents should differ between LM and ILV in the same MVB, but the dynamics within tetraspanin networks and between tetraspanins and associated proteins are at present unknown. To visualize these dynamics in living cells requires techniques with sufficient resolution to detect the different subdomains. At the same time, these techniques should allow detection of the position of the various molecules relative to one another. For these reasons, we applied confocal Fluorescence Resonance Energy Transfer (FRET) technology with different combinations of CFP- or YFP-tagged MHC-II (HLA-DR3), DM and the tetraspanin CD63 and CD82 proteins. After verification of correct localization of the fluorescently tagged molecules by immuno-electronmicroscopy, we performed confocal FRET (van Rheenen et al., 2004) on vesicles neutralized and expanded by chloroquine to distinguish ILV from LM by light microscopy as MVB are too small to distinguish LM from ILV on live unfixed cells (Zwart et al., 2005). We tested various combinations of MHC-II and DM with CD63 and CD82 to show that the orientation of CD63 and CD82 alters in the two different MVB domains, as does their interaction with MHC-II and DM. These experiments are the first to reveal dynamics within the tetraspanin web on subdomains in one compartment, the late endosomal MVB. These data suggest a model explaining dynamic and selective interactions of tetraspanins with associated molecules DM and MHC-II within MVB subdomains, which may occur for other tetraspanin-associated proteins as well.

Results

Expression of MHC-II and Tetraspanin in MelJuSo and HEK293T cells

MHC-II expression is limited to Antigen Presenting Cells (APC), such as dendritic cells, macrophages, B-cells and monocytes. These primary cells are

difficult to manipulate genetically and photosensitive, which complicates live-cell fluorescence microscopy. We therefore set up a reconstituted model cell system by stably expressing the relevant molecules in Human Embryonic Kidney (HEK) cells. HEK293T were used to introduce Ii along with YFP-tagged MHC-II (HLA-DRB3 with non-fluorescent HLA-DRA) alone or in combination with CFP tagged DM (Table S1 includes a description of all stably transfected cell lines used). To show proper formation of MHC-II complexes, we performed flow cytometry with antibodies recognizing MHC-II/peptide or MHC-II with the remaining Ii-derived CLIP fragment and compared the expression with the endogenously MHC-II expressing melanoma cell line MelJuSo (Fig. S1A). MHC-II molecules were efficiently expressed and presented CLIP fragments when DM was absent, as described before (Avva and Cresswell, 1994).
We also introduced CFP- or YFP- tagged CD63 or CD82 molecules in HEK293T cells. The tetraspanins were C-terminally tagged to avoid interference with the lysosomal targeting signal (Blott et al., 2001). Localization of endogenously expressed or ectopically expressed fluorescently tagged tetraspanins was determined using confocal laser scanning microscopy (CLSM) and electronmicroscopy (Figs S1B, 3). Similar to endogenous tetraspanins, YFP-CD63 or -CD82 localized to intracellular compartments and to the cell surface. To determine the relative levels of endogenously versus ectopically expressed CD63 or CD82, we analyzed the cells by SDS-PAGE and Western blotting considering the additional molecular weight contributed by the YFP tag (Fig. S1C). Tetraspanins have extensive carbohydrate chains, which generate multiple bands by SDS-PAGE. Still, ectopically expressed fluorescently tagged CD63 constitutes more than half of the total CD63 pool and the ectopic fluorescently tagged CD82 pool constitutes considerably more than the endogenous CD82 expressed in HEK293T cells. Relatively high expression of CFP- or YFP-tagged molecules over endogenous molecules is essential to achieve a reasonable amount of fluorescent pairs for FRET detection as pairing with endogenous non-fluorescent molecules will quench the FRET signal.
In conclusion, we introduced the tetraspanins CD63 and CD82 as well as MHC-II and DM in a fluorescent form in HEK293T cells, thereby creating a model to study the dynamics of the MHC-II/DM interactions within the context of tetraspanin networks in MVB of living cells.

Lateral movement of tetraspanins and HLA-DR in the plasma membrane
Proteins diffuse in lipid bilayers at rates dependent on their radius in the membrane according to the Saffman-Delbruck equation $D=cT\ln[(k/ha)-0.05772]$ where D is diffusion in the membrane, c and k are constants, T is absolute temperature, h is viscosity of the membrane and a is the radius of the transmembrane segments (Reits and Neefjes, 2001; Saffman and Delbruck, 1975). Consequently, large protein complexes such as tetraspanin proteins diffuse slower than smaller ones, but the diffusion rates of MHC-I and MHC-II, that consist of one and two transmembrane regions respectively, will be almost similar. However, molecules will diffuse at slower rates when interacting with larger complexes that are less mobile, as can be assessed by Fluorescence Recovery After Photobleaching (FRAP) technology. In a FRAP experiment, a small region in the cell is bleached

and the recovery of fluorescence by diffusion from the surrounding membrane area is followed and quantified (Fig. 1A). The resulting fluorescence recovery curve allows determination of (at least) two factors; the immobile fraction and the rate of mobility expressed as $T_{1/2}$ that represents the time required for 50%

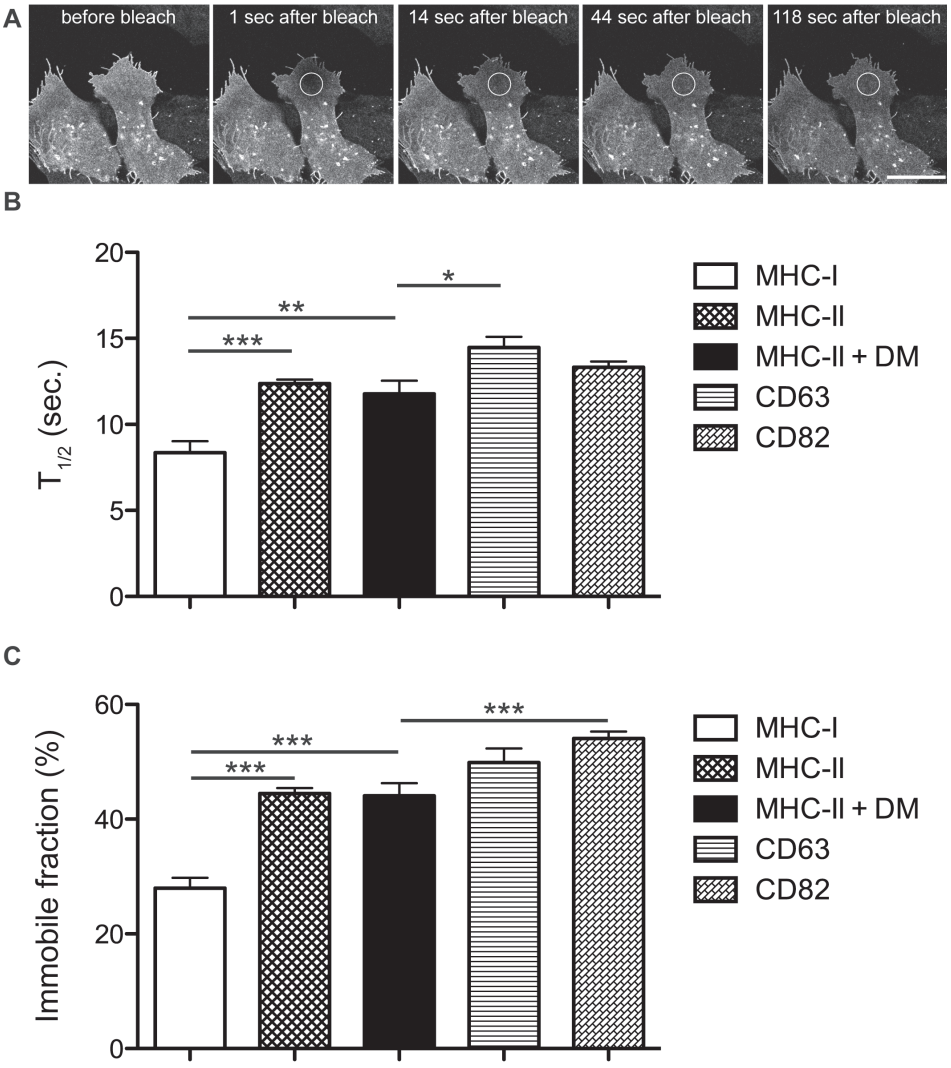

Figure 1: Mobility of fluorescently tagged MHC-I (HLA-A2), MHC-II (HLA-DRB3), CD63 and CD82 at the plasma membrane. HEK293T cells stably expressing CFP-, GFP- or YFP-tagged MHC-I, Ii and MHC-II with or without coexpression of DM - CD63 or CD82 were bleached according to a FRAP protocol to determine the mobility and the mobile fraction of these fluorescent proteins at the plasma membrane. (A) HEK293T expressing YFP-CD63 imaged before and at several time points after point bleach. Fluorescence recovery is measured in a Region Of Interest (ROI) represented by the white ring. Bar: 20 µm. (B) Mean mobility as $T_{1/2}$ values (seconds) and (C) immobile fractions (percentage of initial fluorescence in the bleach spot) for fluorescently tagged MHC-I (n=15), MHC-II (n=33), MHC-II in the presence of DM (n=12), YFP-CD63 (n=27) and YFP-CD82 (n=22) expressed in HEK293T cells are shown. Error bars represent SEM and *P<0.05, **P<0.01, ***P<0.001 (students t-Test).

recovery of the mobile fraction (Fig. S2 (Reits and Neefjes, 2001)).

Tetraspanins have four transmembrane regions (TMs) and may assemble into large protein networks, which would result in slow lateral mobility. Peptide- or CLIP-loaded MHC-II HLA-DR3 $\alpha\beta$ complexes contain two transmembrane regions. MHC-I HLA-A2-GFP – introduced as a control molecule - contains one transmembrane region only (Gromme et al., 1999). We performed FRAP experiments on HEK293T cells expressing YFP-CD63, YFP-CD82 or CLIP-loaded HLA-DRB-YFP. Furthermore, a potential interaction may differ between CLIP-loaded and proper peptide-loaded MHC-II molecules. Therefore, we introduced DM to perform FRAP on peptide-loaded HLA-DRB-YFP as well (for stable cell lines, see Table S1). Both peptide- and CLIP-loaded MHC-II moved considerably slower than MHC-I, and diffused at rates similar as CD63 or CD82. The immobile fraction for MHC- I was also smaller than for MHC- II or tetraspanins (Figs 1B, 1C). This suggests that MHC- II resides in larger protein complexes at the plasma membrane than MHC-I. These complexes may contain tetraspanins that have similar diffusion characteristics in living cells.

Considerations on FRET studies of proteins in MVB

Although similar FRAP characteristics may suggest an association between MHC class II and tetraspanin molecules CD63 and CD82, it certainly does not prove it. To visualize incorporation of HLA-DR and DM in tetraspanin webs containing CD63 and CD82, we measured Fluorescence Resonance Energy Transfer (FRET) between the CFP and YFP tagged molecules in various combinations. When two fluorophores are approximately within a distance of 100 Å, which usually implies direct interactions, FRET may be detected. Collisional FRET can occur by excessive overexpression of two fluorescently tagged proteins. We performed immuno-electronmicroscopy to assess this. Double labelling of fluorescently tagged (anti-GFP) versus the total pool of CD63 or CD82 (anti-CD63 or anti-CD82) does not concur with excessive overexpression of fluorescently tagged over endogenous expressed tetraspanins (Fig. 2). Also labelling MHC-II (anti-DR) and DM (anti-HLA-DM) in the HEK293T transfectants suggest modest ectopic expression levels (Fig.2). The observed labelling intensities (even considering a detection efficiency of approximately 10% in EM slides) and the fact that the CFP/YFP molecules did not show any clustering in the fixed EM sections, excludes collision FRET as a major factor contributing to our detected signals. Of note, our aim is to detect relative alterations in FRET when molecules redistribute within MVB and such differences would not concur with collision as an explanation for FRET signals. FRET is highly sensitive to the distance as well as to the orientation of the two fluorophores. This implies that differences in FRET do not necessarily reflect differences in distance, but could equally well indicate an altered orientation of the fluorescent tags or a combination of the two. However, a bona fide FRET signal always reflects close local approximation of the two molecules.

To determine FRET on membranes of MBV, high resolution data were collected using a confocal scanning light microscope (CSLM) followed by calculation of sensitized emission FRET (seFRET) (van Rheenen et al., 2004). The MVB

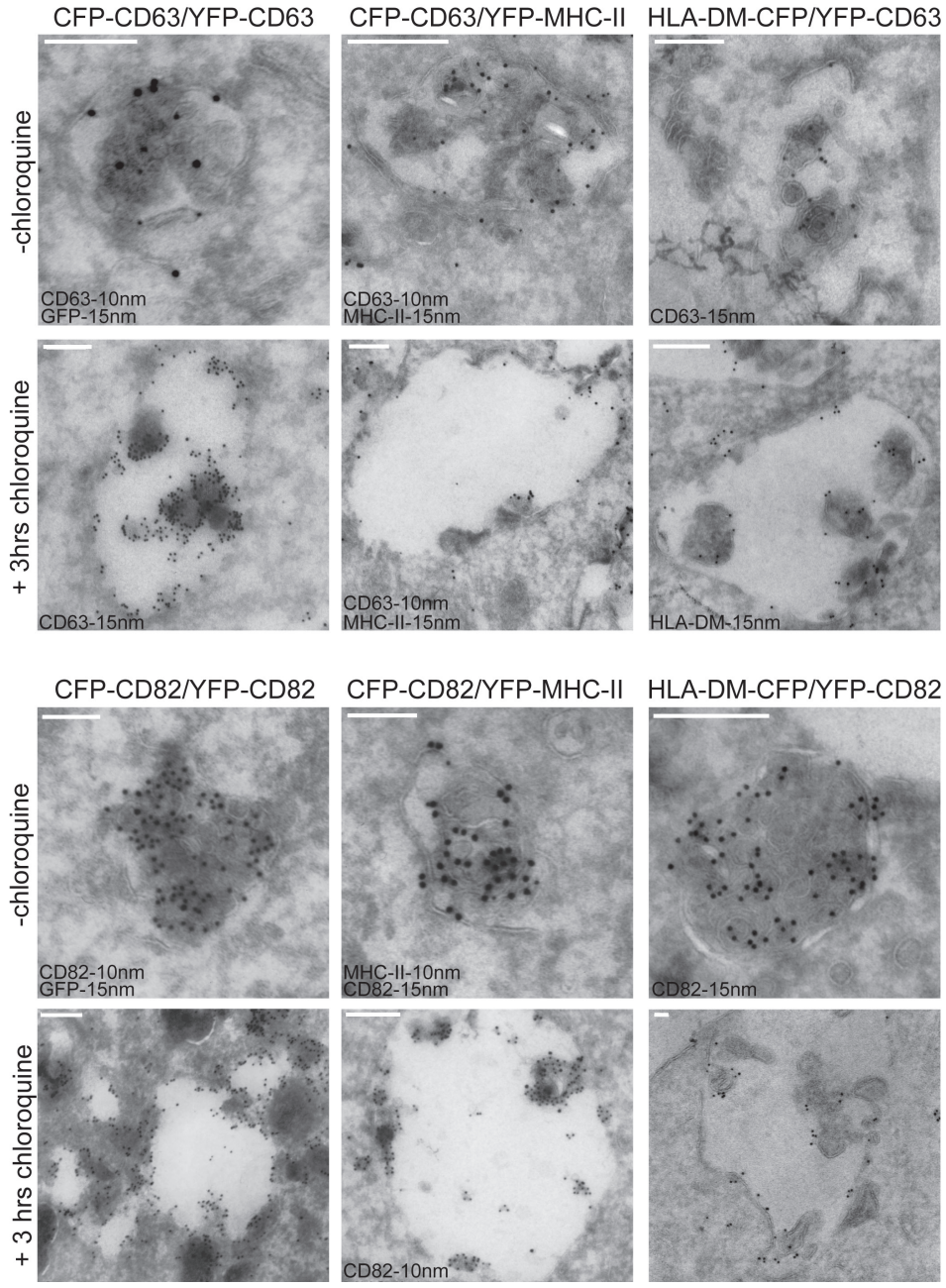

Fig. 2: Distribution of CFP- or YFP-tagged CD63, CD82, HLA-DM and MHC-II (HLA-DR) in multivesicular bodies. Electron micrographs of stable HEK293T cell transfectants expressing YFP and CFP-CD63, YFP and CFP-CD82, CFP-CD63 or CFP-CD82 together with MHC-II-YFP and HLA-DM-CFP together with YFP-CD63 or YFP-CD82, as indicated. Cells were fixed before (-) or after three hours of chloroquine treatment and cryo-sections were stained with anti-GFP, anti-CD63, anti-CD82, anti HLA-DM and anti HLA-DR antibodies and gold particles for detection by EM, as indicated. Representative images of control or chloroquine treated (partially swollen) multivesicular bodies (MVBs) are shown. Bar (white): 500 nm.

containing MHC-II and DM are around 400nm in diameter, which does not allow separation of ILV and LM within these structures by conventional light microscopy. To overcome this, cells were exposed to chloroquine that neutralizes and swells the MVBs. Swelling is the result of fusion of ILV with the LM of MVB, thus providing the membranes required for the extension of the LM. In addition, the markers on ILV relocate to the LM under these conditions.
Swelling of MVB is a relatively slow process. After exposure of cells to chloroquine for three hours, the MVBs are partially swollen with some ILV still present in the expanded MVB. This condition allows visualization of both subdomains in one MVB by CLSM. Full expansion of MVB at the cost of ILV takes about six hours of chloroquine exposure in HEK293T cells, as visualized in Fig. S3.

Location of proteins in MVB by cry-immuno-electronmicroscopy
To show the location of the various CFP- or YFP-tagged proteins within normal and partially swollen MVBs by chloroquine exposure, we analyzed the double transfectants by cryo-immuno-electronmicroscopy (Fig. 2). We analyzed various conditions: the control situation and the cells after three hours of chloroquine exposure. We used this condition to expand the vesicles to separate ILV and the LM for light microscopy, which has a maximal resolution of around 200 nm while normal MVB have a radius of ~400 nm preventing separation of ILV from LM. This protocol of swelling MVB to resolve the two subdomains of MVB by light microscopy and has been used before to detect MHC-II interactions with DM in the subdomains of MVB (Zwart et al., 2005). Sections of the HEK293T cells were labelled with anti-GFP antibodies and further probed with gold particles. The ILV of most MVB labelled for the proteins indicated and chloroquine exposure yielded swollen structures with internal vesicles still labelled for the CFP/YFP-tagged proteins.

Effect of neutralizing MVB on FRET signals
To investigate whether MHC-II and DM reside in tetraspanin webs containing CD63 and CD82, we generated cells with different combinations of tetraspanins and MHC-II or DM molecules. The fluorescent tag always localizes to the cytosol or the interior of ILV (which is topologically identical). Since we have to manipulate the cells with chloroquine to expand the MVB for analyses by CLSM, we tested the effects on FRET between the two proteins. Chloroquine diffuses almost instantaneously over membranes, causing neutralization of acidic compartments including MVB. We exposed cells to chloroquine for ten minutes (when MVB swelling is not detected) before FRET was measured. Neutralization of MVB by chloroquine did only have a minor effect on FRET values between the protein pairs tested. For instance, FRET values between a fluorescently tagged CD82-CD82 pair showed a subtle increase, while only a small decrease for the CFP-YFP tagged CD63-CD63 pair was observed following neutralization of MVB (Fig. S4A). Since chloroquine exposure yielded different effects for the various FRET-pairs tested, the effects are not due to pH (which is clamped by chloroquine at ~pH 7.0), but indicate pH dependent reorganization of complexes. To compensate for effects of pH on FRET values between our protein pairs, we relate FRET values measured on swollen MVBs to FRET values obtained after ten minutes

chloroquine exposure of cells.

Controlling vesicle movement for accurate confocal FRET measurements
For confocal FRET measurements, the sample is excited at 430 nm light and donor fluorescence and acceptor fluorescence (the actual FRET) emission is measured. This is followed by excitation with light of 514 nm to measure acceptor fluorescence emission. From these three data sets, FRET and donor FRET efficiency (E_D: FRET related to donor fluorescence, which reflects the efficiency of donor fluorophores to transfer energy) are calculated. As we are working at maximal resolution, the MVBs in the living cells should not move between the images made for determining FRET, which takes five milliseconds as we are calculating the amount of signals per pixel. Chemical fixation is no alternative, as fixation will unpredictably affect the protein complexes. Immediate elimination of all microtubule-based transport by high concentrations of nocodazole was not sufficient (the vesicles still showed some 'trembling', not shown) and induced apoptosis of the cells.
We then decided to perform FRET measurement on cells at 19°C instead of 37°C. We monitored vesicle motion at different temperatures and detected sufficient quenching of vesicle motion at temperatures below 19°C to allow adequate and reliable FRET measurements at our level of resolution. To test whether FRET is affected by lowering the temperature, we measured FRET between CFP- and YFP-CD63 at temperatures between 19°C and 37°C and observed marginal effects on FRET (Fig. S4B). FRET measurements of living cells at 19°C yielded more accurate data at high magnification with minor effects on calculated FRET values. We used this condition to measure differences in FRET either between tetraspanin proteins CD63 and CD82 and interacting proteins DM and MHC-II.
In summary, CLSM data of cells for FRET determination were acquired at 19°C. FRET values were calculated as described (van Rheenen et al., 2004). Discrimination between MVBs either containing or lacking ILV (mainly consisting of LM) was achieved by comparing FRET on vesicles in cells exposed to chloroquine for ten minutes (normal ILV containing neutral MVB) or six hours (maximal expanded MVB without ILV), respectively. These conditions were used for data acquisition, allowing statistical sound statements. For illustration, we included images of cells exposed to chloroquine for three hours yielding partially swollen MVBs with some internal vesicles sufficiently separated from the LM for detection by CLSM.

CD63 and CD82 form homo- and heteromeric interactions *in vivo*: the tetraspanin-web
Using the methods and considerations described above, we measured FRET between CFP- and YFP-tagged CD63 or CD82 molecules and between CFP-CD63 and YFP-CD82 molecules stably expressed in HEK293T cells. Sensitize emission FRET was determined and related to the donor fluorescence yielding E_D. Whereas E_D of the CD63-CD82 pair was similar at ILV and the LM, it was increased for the CD63-CD63 and CD82-CD82 pairs at the LM of the expanded MVB (Fig. 3). These data suggest that the CD63-CD82 core is unaltered at limiting and internal membranes of MVB, whereas CD63-CD63 and CD82-CD82

pairs reposition at the LM of an expanded MVB. Although the exact repositioning in molecular terms cannot be deduced from FRET studies, since the selective contribution of distance and orientation cannot be separated, these results show that tetraspanin webs are dynamic within one structure; the MVB.

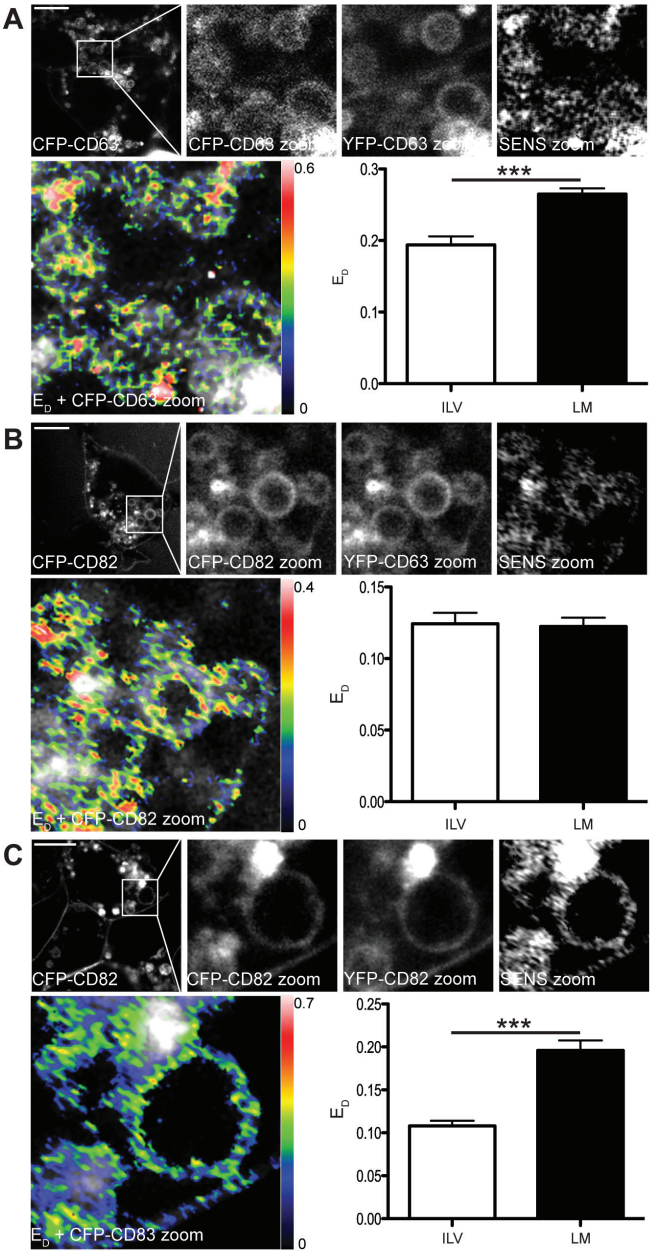

Figure 3: FRET between fluorescently tagged CD63 and CD82.
Sensitize emission (se) FRET was measured in HEK293T cells stably expressing (A) CFP-CD63/YFP-CD63 (B) CFP-CD82/YFP-CD63 and (C) CFP-CD82/YFP-CD82. Microscopic images represent HEK293T cells with expanded MVB to discriminate ILV and LM three hours after chloroquine incubation. Top left; overview of CFP images with zoom-in for CFP and YFP channel, as indicated. The SENS zoom image indicates the calculated seFRET after leak through correction. The overlay shows the calculated donor FRET efficiency E_D in rainbow colours (rainbow bar at right) representing the E_D values per pixel and projected onto the zoom-in of the CFP channel in white colours. Bar: 10 µm. The bar diagrams in the right bottom indicate the calculated E_D values for the interactions between the different tetraspanins at the luminal vesicles (LV, after ten minutes chloroquine) and limiting membrane (LM, after six hours chloroquine). (A) CFP-CD63 and YFP-CD63 pair; n=129 for ILV and n=59 for LM (B) CFP-CD82 and YFP-CD63 pair: n(ILV)=9; n(LM)=34 (C) CFP-CD82 and YFP-CD82 pair: n(ILV)=43 and n(LM)=73. Error bars represent SEM; ***P<0.001 (student t-Test).

Tetraspanin CD63 – unlike CD82 - stably interacts with MHC-II HLA-DR at LM and ILV.

HLA-DR interacts with various tetraspanins, including CD63 and CD82, in biochemical studies (Hammond et al., 1998; Tarrant et al., 2003). To verify this interaction in living cells and to determine spatial differences within the MVB, CFP-CD63 or CFP-CD82 were co-expressed with YFP-MHC-II (HLA-DR3) and Ii in HEK293T cells. Donor FRET Efficiency E_D was determined on MVB from HEK293T cells exposed to chloroquine for ten minutes or for six hours (Fig. 4). Whereas the CD63 - MHC-II interaction was stable between the two states, the interaction between CD82 and MHC-II observed on the LM collapsed at the ILV. Slightly expanded MVB imaged after three hours of chloroquine incubation illustrate the detected differences in E_D for ILV and LM within one MVB. These MVBs still contain some internal structures, as detected in the zoom-ins of the CFP and YFP channels and the projection of E_D (in rainbow colours) on the CFP-image (in white). Most internal vesicles containing CD82 and MHC-II did not yield any E_D signal, in accordance with the quantification of E_D for the two states of MVB. Some cells expressed sufficient levels of CD82 and MHC-II at the plasma membrane for FRET determination, which yielded FRET efficiencies comparable to values detected for the limiting membrane (results not shown). These results indicate that HLA-DR interacts with CD63 on both domains of MVB while CD82

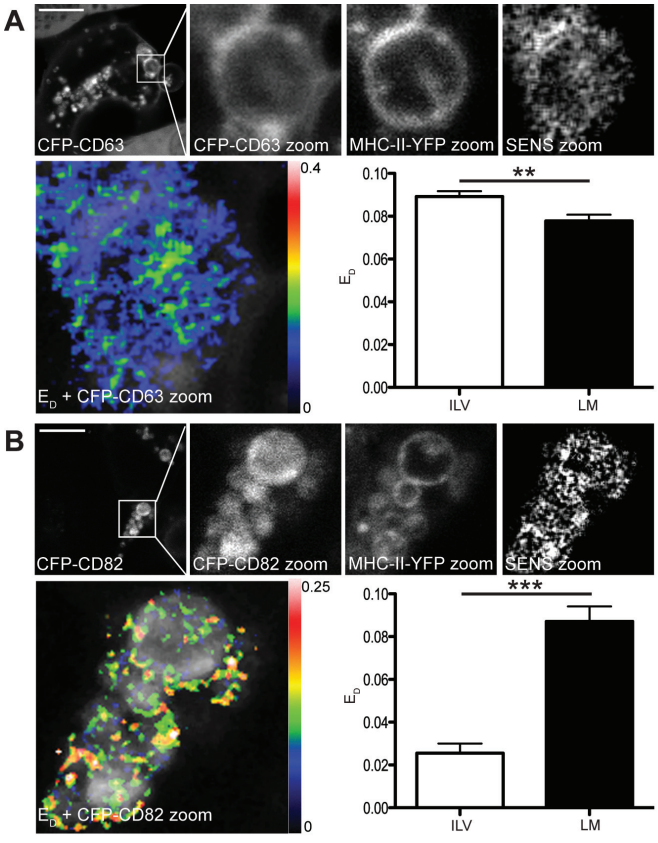

Fig. 4: seFRET between MHC-II HLA-DRB3-YFP and tetraspanins CFP-CD63 or CFP-CD82. FRET measurements and detection as in Fig. 4 but now for HEK293T cells expressing the FRET pairs CFP-CD63 and MHC-II-YFP (A) or CFP-CD82 and MHC-II-YFP (B) with non-fluorescent invariant chain and DM. Bar: 10 µm. The calculated donor FRET efficiencies (E_D) were (A) CFP-CD63 and MHC-II-YFP pair: n(ILV)=127 and n(LM)=158 (B) CFP-CD82 and MHC-II-YFP pair: n(ILV)=43 and n(LM)=73. Error bars represent SEM; **P<0.01, ***P<0.001 (student t-Test).

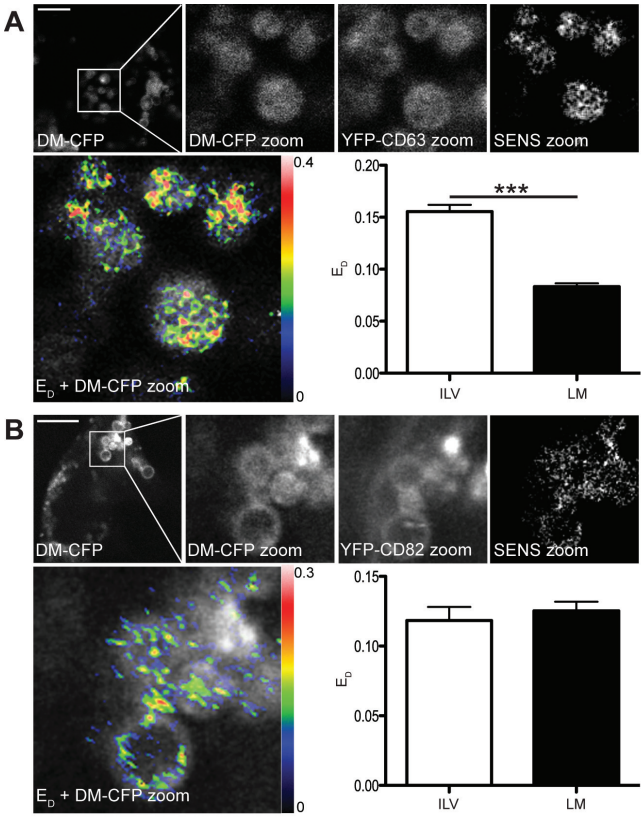

Fig. 5: seFRET between DM-CFP and tetraspanins YFP-CD63 or YFP-CD82. FRET measurements and detection as in Fig. 4 but now with HEK293T cells expressing the FRET pairs (A) YFP-CD63 and DM-CFP or (B) YFP-CD82 and DM-CFP. Bar: 10 µm. The calculated donor FRET efficiencies (E_D) were (A) DM-CFP and YFP-CD63 pair; n(ILV)=80 and n(LM)=111, (B) DM-CFP and YFP-CD82: n(ILV)=49 and n(LM)=96. Error bars represent SEM, **P<0.01, ***P<0.001 (student t-Test).

re-orientates or enters the network at the limiting membrane of MVB and possibly also at the plasma membrane.

Tetraspanin CD82 – unlike CD63 - stably interacts with DM at LM and ILV. Since DM and MHC-II primarily pair at the ILV (Zwart et al., 2005), we wondered how DM would interact with the tetraspanins CD63 and CD82 at ILV and LM. We expressed CFP-tagged DM and YFP-CD63 or YFP-CD82 in HEK293T cells and measured donor FRET efficiency E_D on chloroquine-control or -expanded MVB (Fig. 5). CD82 associated with DM in a stable fashion and equal orientation while CD63 yielded highest E_D in the ILV, rather than the LM of MVB. This situation differed considerably for the interaction of tetraspanins with MHC-II that stably interacted with CD63 while CD82 only interacted with MHC-II at the LM of MVB (Fig. 4) and suggests reorientation of MHC-II and DM within the reorganized tetraspanin network between ILV and LM of one MVB.

Discussion

The family of tetraspanin proteins is fascinating, as they are major constituents of endosomes and still poorly understood. Although some tetraspanins are expressed at the plasma membrane, many accumulate in late endosomal

MVB. The EM structure of the uroplakin tetraspanin network shows a highly ordered protein network in membranes; the tetraspanin web (Min et al., 2003). Other tetraspanin family members may assemble in similar structures, but this is unclear. At least six tetraspanin proteins – including CD63 and CD82 - are located in late endosomal MVB and are enriched in the internal luminal vesicles (ILV) (Escola et al., 1998; Peters et al., 1991; Wubbolts et al., 2003). Although it is unclear whether these tetraspanins form proteinaceous networks in MVB, biochemical studies have shown that they can be co-isolated with MHC-II, DM and other molecules residing in MVB (Hammond et al., 1998). Biophysical studies have shown that MHC-II and DM interact in the ILV rather than at the LM of MVB (Zwart et al., 2005). This observation was puzzling and suggested that the MHC-II interaction with DM was stabilized in particular microdomains in MVB. Because tetraspanin proteins accumulate at ILV and interact with both MHC-II and DM, the tetraspanin network could act as a stabilizing factor. In mouse DCs, the tetraspanin molecule CD9 clusters two types of MHC-II molecules, I-A and I-E that show a distinctive organization on the plasma membrane. I-A and I-E both interact with CD9 and with each other, which is lost in DC lacking CD9 (Unternaehrer et al., 2007) suggesting a role of tetraspanins in the organization of MHC-II in membranes.

Whether CD63 and CD82 form networks that dynamically interact with DM and MHC-II was investigated in this study. We first measured the mobility of the tetraspanin proteins CD63 and CD82 at the plasma membrane and compared it to mobility rates of MHC-I and -II, which pass the membrane one or two times respectively. MHC-I and -II molecules should move at similar rates according to the Saffman-Delbruck equation. However, MHC-II mobility rates were considerably slower and similar to the four times transmembrane spanning proteins CD63 and CD82 (that may move relatively slow when present in multi-molecular complexes). This could suggest that MHC-II localizes to similar sized complexes. However, these do not necessarily need to be the CD63 or CD82 tetraspanin webs, as diffusion studies do not provide this information. Such conclusions can be drawn by FRET technology, as FRET is only detectable when two fluorophores are within a distance of 100 Å. FRET is highly sensitive to alterations in distance (it decays with r^6) and to changes in the orientation of the fluorophores. FRET is thus the prime technique to determine protein-protein interactions and conformational changes in living cells. We applied FRET to measure interactions and/or orientations between tetraspanins CD63 and CD82 as well as their interaction with MHC-II and DM. MVB were selectively expanded by use of chloroquine to reposition the molecules to the LM to deduce the state of interaction at two MVB locations, the ILV and the LM.

We first determined the interaction, expressed as Donor FRET efficiency (E_D) between two tetraspanin proteins – CD63 and CD82 – when predominantly present at ILV (10 minutes chloroquine) and LM (after 6 hours chloroquine). The interaction between CD63 and CD82 appeared to be very stable (same E_D), whereas CD63-CD63 and CD82-CD82 pairs had lower Donor FRET efficiency at the ILV of the MVB. This does not necessarily imply fewer protein-protein interactions, but could also reflect a different orientation of the proteins in the ILV and on the LM. It implies that different tetraspanin proteins interact within the

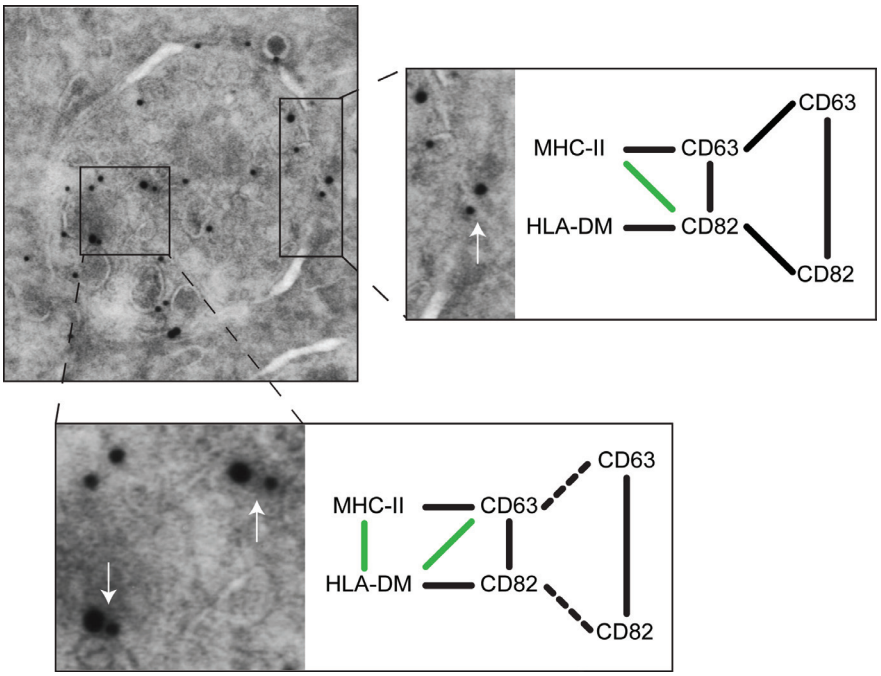

Fig. 6: Schematic representation of the reorganization of the MHC-II loading complex within tetraspanin domains within the multivesicular bodies. A micrograph showing a MVB from MelJuSo cells double labelled for MHC-II (MHC-II, 10 nm gold) and CD63 (15 nm gold). The white arrow shows MHC-II and CD63 closely locating on LM and ILV respectively. The box around ILV and the box around a segment of the LM connect to a schematic representation of the different tetraspanin interactions with MHC-II and DM detected by FRET in the two subdomains of MVB. Interactions that differ in the two MVB subdomains are highlighted in green. The interactions between CD63-CD63 and CD82-CD82 differ between LM (solid line) and ILV (dashed line) while the CD86-CD63 interaction does not differ. Bar: 200 nm.

MVB and that these tetraspanin interactions are dynamic at the different MVB subdomains. This is illustrated by different E_D values for the CD63 and the CD82 pairs. The stable CD63-CD82 interaction might function as a core enabling other CD63 and CD82 molecules to interact and diffuse in a dynamical fashion.

Although FRET resolves protein–protein interactions at a very high resolution, it is difficult to measure more than one pair using genetically encoded fluorophores. To study the interaction of DM or MHC-II with tetraspanins, we had to generate various cell lines containing all combinations. We determined donor FRET efficiency as we have done for the different tetraspanin pairs. Again, we observed marked differences for tetraspanin interactions with MHC-II or DM within the MVB. MHC-II interacted stably with CD63, but CD82 only showed FRET with MHC-II at the LM. DM interacted stably with CD82 whereas the MHC-II/CD63 pair showed strongest E_D at the LM of MVB. In addition, DM and MHC-II preferentially interacted at the ILV within MVB (Zwart et al., 2005). How to build a model from these dynamic FRET interactions?

When plotting all possible interactions (Fig. 6), several points stand out. At the ILV,

DM interacts with CD63 and MHC-II while these molecules are repositioned at the LM of MVB where CD82 interacts with MHC-II and DM. MHC-II and DM only pair in the ILV, as determined by FRET. Whether CD63 is critical for stabilizing this interaction, is unclear. Silencing CD63 does not affect antigen presentation by MHC-II but may be compensated, as we observed that cells immediately overexpress CD82 in response (unpublished observations). It is possible that various tetraspanin networks, including tetraspanins expressed in immune cells such as CD9, CD37, CD51, CD63, CD81 and CD82 (reviewed in (Tarrant et al., 2003)) are able to cluster MHC-II and DM in ILV to create a proteinaceous subdomain for successful antigenic peptide loading.
It is unclear why tetraspanin networks would reorganize at the ILV or LM of the MVB. The lipid and protein content of the two MVB subdomains is different. ILV concentrates the lipids LBPA and cholesterol (Kobayashi et al., 1998; Matsuo et al., 2004), which may contribute to the assembly of the tetraspanin networks. Proteins are also unevenly distributed over the two MVB subdomains, as illustrated by the tetraspanins that accumulate in ILV (Escola et al., 1998). Finally, the curvature of ILV is definitively different from the curvature of the LM of the same MVB, which may affect formation of particular (lipid-) protein complexes (Mukherjee and Maxfield, 2000). We show for the first time that tetraspanin networks are dynamic within one subcellular structure by applying FRET technology. The cause and consequences thereof still have to be defined. One consequence appears to be the stabilization of DM and MHC-II complexes, which only occurs in ILV. The altered positioning of DM and MHC-II on the LM might explain the failure of MHC-II antigen presentation on phagosomal (limiting) membranes that surround intracellular bacteria (Zwart et al., 2005).
The observations from our FRET studies, where we followed the tetraspanin network and two associated proteins, suggest that tetraspanin networks reorganize at different locations within MVB. In the ILV, the interaction between MHC-II and DM is stabilized, probably by CD63 that interacts with both molecules. At the LM of the MVB, DM appears to prefer CD82. MHC-II automatically positions itself differently within this tetraspanin network and the contact with its chaperone DM may loosen. The reorganization of the tetraspanin networks in MVB may re-orientate associate proteins in unfavourable positions resulting in inefficient MHC-II peptide loading at the limiting membrane of MVB (Zwart et al., 2005).

Materials and Methods

DNA Constructs and the Generation of Transfectants

To generate pCFPC1-CD63 and pYFPC1-CD63, we retrieved CD63 from an GFP-CD63 fusion construct (Blott et al., 2001) using BamHI-Mlu1 and placed CD63 into peCFP-C1 (Clontech), peYFP-C1 (pYFP-C1 was generated by exchange of CFP from peCFP-C1 for YFP (Miyawaki et al., 1997; van Rheenen et al., 2004)), pmCFP-C1 and pnCitrine-C1. To generate pCFPC1-CD82, pYFPC1-CD82, CD82 was amplified from image clone 2959683 using CD82 forward primer GAAGATCTATGGGCTCAGCCTGTATCAAA and CD82 reversed primer CGGAATTCTCAGTACTTGGGGACCTTG and was ligated into peCFP-C1 and peYFP-C1 using BglII-EcoRI. pcDNA3-p31Ii was a kind gift from Dr. O. Bakke

(Bakke and Dobberstein, 1990). pcDNA3.1 Zeo DMβ-IRES-DMα/YFP, pcDNA3 DRα-IRES-DR3β/CFP pcDNA3-H2B/CFP and -H2B/YFP were already described (Zwart et al., 2005).

Antibodies
Monoclonal antibodies: anti-CD63 (NKI-C3) (Vennegoor and Rumke, 1986), anti-CD82 (C33) (Fukudome et al., 1992; Imai et al., 1992), anti-DMA (5C1) (Sanderson et al., 1996), L243 and anti CerCLIP.1 were isolated from hybridoma cell lines L243 (anti-HLA-DR complex, ATCC) and CerCLIP.1 (anti-CLIP24) have been described previously (Denzin et al., 1994; Lampson and Levy, 1980). Rabbit polyclonal anti-GFP (Rocha et al., 2009), anti-HLA-DR (Neefjes et al., 1990) and anti-human CD63 (NKI-C3 serum) were used.

Cell lines
The different stable HEK293T cell lines generated for this study are listed in Table S1. Cells were cultured in DMEM (Gibco) supplemented with 7.5% fetal calf serum (Gibco) in the presence or absence of 1000 µg/ml G418, 300 µg/ml Hygromycin (Gibco), 500 µg/ml Zeocine (Invitrogen) and/or 2µM Ouabaine (Invitrogen) at 37°C in a humidified atmosphere containing 5% CO2. Stable and homogeneous expression of CFP- and YFP-tagged proteins was ensured by regular selection of the CFP- and YFP-positive cells by FACS sorting. Stable transfectants of the melanoma cell line MelJuSo (H2B-CFP, H2B-YFP) were grown in IMDM (Gibco) medium with 7.5% FCS supplemented with 1000 µg/ml G418 (Gibco).

Flow Cytometry of Cell surface MHC-II
HEK293T cells transfected with the various constructs or MelJuSo cells were harvested from culture plates using trypsin-EDTA (Gibco) collected in PBS supplemented with 2% fetal calf serum. Cells were incubated with primary antibodies L243 and CerCLIP.1 at 4°C for 45 minutes. After two additional washes, cells were incubated with secondary antibody Goat anti-Mouse-Alexa-647 (Invitrogen) at 4°C for 30 minutes. After three washes, cells were analyzed by a FACS calibur (Becton Dickinson).

CLSM and Cryo-Immuno-electronmicroscopy Analysis
For CLSM analysis, coverslips were coated with 5 µg/ml fibronectin (Sigma-Aldrich co.) in PBS for 1h at 37°C. Subsequently, HEK293T transfectants were seeded on the coated coverslips. Cells were fixed by a 3.75% formaldehyde solution (free from acid, Merck) in PBS and stained with anti-CD63 antibodies (NKI-C3) and anti-CD82 antibodies (C33) and secondary antibodies conjugated to goat-anti-mouse Alexa-647. Images were taken with a Leica TCS SP2 System (Leica).
HEK293T transfectants were incubated with 200µM chloroquine three hours before processing. Cells were fixed in a mixture of paraformaldehyde (2%) and glutaraldehyde (0.2%) in 0.1 M PHEM buffer (60 mM PIPES, 25 mM HEPES, 2 mM MgCl2, 10 mM EGTA, pH 6.9) prior to processing for cry-immuno-electronmicroscopy. For immuno-labeling, sections were incubated with purified mAb anti-human HLA-DMα (5C1), or mAb anti-human CD82 (C33) and followed

by incubations with Rabbit-anti-Mouse IgG and protein A-conjugated 10nm or 15 nm colloidal gold (EM Lab, Utrecht University, Netherlands). For double labelling, the sections were fixed again for 10 min. with 1% glutaraldehyde, followed by a second incubation with rabbit-anti-GFP, rabbit anti-human HLA-DR serum or rabbit anti-human CD63 (NKI-C3) serum followed by labelling with protein A-conjugated 10nm or 15nm colloidal gold. After embedding in a mixture of methylcellulose and uranyl acetate, sections were analyzed in a Philips CM10 electron microscope (Eindhoven, the Netherlands)

FRAP

FRAP experiments were performed with a Leica TCS SP2 System (Leica) with AOBS controlled emission using a 63x oil lens with a temperature controlled culture device. Focussing on the basal plasma membrane, a region of interest (ROI) was chosen and bleached at maximum power for 1s at zoom four for one second returning to 5% laser power for subsequent imaging. First, five pictures (at 512*512 resolution) were taken with time intervals of 1.6 seconds to measure the fluorescence before bleaching F_i. Then a bleach-point was set in the middle of a cell. Reappearance of fluorescence until (F_∞) in the bleach spot area was measured over a period of approximately eight minutes.

The immobile fraction and the rate of mobility were determined from the fluorescence recovery curve (Fig. S2). The rate of mobility or diffusion time (τ_D) is the time-period required for recovery of 50% of the fluorescence of the mobile fraction. The immobile fraction (I) is calculated by the equation $I = (F_i – F_\infty)/ (F_i)$, where F_i represents the fluorescence before bleaching and F_∞ the recovered fluorescence in the bleach spot area after bleaching at t is infinite (Reits and Neefjes, 2001).

Confocal FRET (CLSM-FRET) Imaging for Sensitized Emission FRET

The HEK293T transfectants were grown on coated coverslips for 72h before imaging. 16h prior to imaging, MelJuSo cells stably transfected with H2B-CFP or H2B-YFP (as internal calibration standards for leak-through and laser fluctuation), were added to the culture as detailed before (van Rheenen et al., 2004). Cells on coverslips were analyzed by CLSM in a heated tissue culture chamber at 37°C and in a cooled tissue culture chamber at 19°C under 5% CO_2. Prior to CLSM analysis, culture medium was exchanged for 3 ml heated (37°C) or cooled (4°C) CBS medium (140 mM NaCl, 5 mM KCl, 2 mM $MgCl_2$, 1 mM $CaCl_2$, 23 mM $NaHCO_3$, 10 mM D-Glucose, 10mM Hepes pH 7.3). When indicated, chloroquine was added at a final concentration of 200 µM for ten minutes, three hours or six hours prior to analyses. For the samples left untreated or incubated for six hours with chloroquine at 37°C nocodazole (3 mM final concentration) was used to block intracellular vesicle motility.

Fluorescence Resonance Energy Transfer between CFP and YFP molecules was studied by calculating the sensitized emission (the YFP emission upon CFP excitation) from separately acquired donor and acceptor images. Images were acquired on a DM-Ire2 inverted microscope fitted with a TCS-SP2 scanhead (Leica). Three images were collected: CFP excited at 430nm and detected between 470 and 490nm; indirect YFP excited at 430 nm and detected between

528 nm and 603 nm; and direct YFP excited at 514 nm and detected between 528 nm and 603 nm.
Because of considerable overlap of CFP and YFP spectra, YFP emission was corrected for leak-through of CFP emission and for direct excitation of YFP during CFP excitation using the co-cultured MelJuSo cells expressing only H2B-CFP or H2B-YFP as internal standards. FRET was calculated from these data as described in detail (van Rheenen et al., 2004). Sensitized emission (FSen) was calculated using correction factors obtained from cells expressing either CFP or YFP alone, which were updated for every image. Then the donor FRET efficiency E_D was determined by relating the FSen to donor fluorescence level on a pixel-by-pixel basis.

Acknowledgements

This study was supported by grants from the Dutch Cancer foundation Koningin Wilhelmina Fonds (KWF) and the Dutch organization for scientific research NWO-ALW (815.02.009). We are grateful to K. Jalink for introducing us into confocal FRET measurements and for critical suggestions on the manuscript, M. J. Jongsma for design of Fig. 6, A. Griekspoor for design of Fig. S3 and P. Paul for critical reading of the manuscript.

References

Avva, R.R., and Cresswell, P. (1994). In vivo and in vitro formation and dissociation of HLA-DR complexes with invariant chain-derived peptides. Immunity *1*, 763-774.

Bakke, O., and Dobberstein, B. (1990). MHC class II-associated invariant chain contains a sorting signal for endosomal compartments. Cell *63*, 707-716.

Blott, E.J., Bossi, G., Clark, R., Zvelebil, M., and Griffiths, G.M. (2001). Fas ligand is targeted to secretory lysosomes via a proline-rich domain in its cytoplasmic tail. J Cell Sci *114*, 2405-2416.

Denzin, L.K., and Cresswell, P. (1995). HLA-DM induces CLIP dissociation from MHC class II alpha beta dimers and facilitates peptide loading. Cell *82*, 155-165.

Denzin, L.K., Robbins, N.F., Carboy-Newcomb, C., and Cresswell, P. (1994). Assembly and intracellular transport of HLA-DM and correction of the class II antigen-processing defect in T2 cells. Immunity *1*, 595-606.

Engering, A., and Pieters, J. (2001). Association of distinct tetraspanins with MHC class II molecules at different subcellular locations in human immature dendritic cells. Int Immunol *13*, 127-134.

Escola, J.M., Kleijmeer, M.J., Stoorvogel, W., Griffith, J.M., Yoshie, O., and Geuze, H.J. (1998). Selective enrichment of tetraspan proteins on the internal vesicles of multivesicular endosomes and on exosomes secreted by human B-lymphocytes. J Biol Chem *273*, 20121-20127.

Fukudome, K., Furuse, M., Imai, T., Nishimura, M., Takagi, S., Hinuma, Y., and Yoshie, O. (1992). Identification of membrane antigen C33 recognized by monoclonal antibodies inhibitory to human T-cell leukemia virus type 1 (HTLV-1)-induced syncytium formation: altered glycosylation of C33 antigen in HTLV-1-positive T cells. J Virol *66*, 1394-1401.

Griffiths, G., Hoflack, B., Simons, K., Mellman, I., and Kornfeld, S. (1988). The mannose 6-phosphate receptor and the biogenesis of lysosomes. Cell *52*, 329-341.

Gromme, M., Uytdehaag, F.G., Janssen, H., Calafat, J., van Binnendijk, R.S., Kenter, M.J., Tulp, A., Verwoerd, D., and Neefjes, J. (1999). Recycling MHC class I molecules and endosomal peptide loading. Proc Natl Acad Sci U S A *96*, 10326-10331.

Hammond, C., Denzin, L.K., Pan, M., Griffith, J.M., Geuze, H.J., and Cresswell, P. (1998). The tetraspan protein CD82 is a resident of MHC class II compartments where it associates with HLA-DR, -DM, and -DO molecules. J Immunol *161*, 3282-3291.

Imai, T., Fukudome, K., Takagi, S., Nagira, M., Furuse, M., Fukuhara, N., Nishimura, M., Hinuma, Y., and Yoshie, O. (1992). C33 antigen recognized by monoclonal antibodies inhibitory to human T cell leukemia virus type 1-induced syncytium formation is a member of a new family of transmembrane proteins including CD9, CD37, CD53, and CD63. J Immunol *149*, 2879-2886.

Kobayashi, T., Stang, E., Fang, K.S., de Moerloose, P., Parton, R.G., and Gruenberg, J. (1998). A lipid associated with the antiphospholipid syndrome regulates endosome structure and function. Nature *392*, 193-197.

Kropshofer, H., Arndt, S.O., Moldenhauer, G., Hammerling, G.J., and Vogt, A.B. (1997). HLA-DM acts as a molecular chaperone and rescues empty HLA-DR molecules at lysosomal pH. Immunity *6*, 293-302.

Lampson, L.A., and Levy, R. (1980). Two populations of Ia-like molecules on a human B cell line. J Immunol *125*, 293-299.

Matsuo, H., Chevallier, J., Mayran, N., Le Blanc, I., Ferguson, C., Faure, J., Blanc, N.S., Matile, S., Dubochet, J., Sadoul, R*., et al.* (2004). Role of LBPA and Alix in multivesicular liposome formation and endosome organization. Science *303*, 531-534.

Min, G., Wang, H., Sun, T.T., and Kong, X.P. (2006). Structural basis for tetraspanin functions as revealed by the cryo-EM structure of uroplakin complexes at 6-A resolution. J Cell Biol *173*, 975-983.

Min, G., Zhou, G., Schapira, M., Sun, T.T., and Kong, X.P. (2003). Structural basis of urothelial permeability barrier function as revealed by Cryo-EM studies of the 16 nm uroplakin particle. J Cell Sci *116*, 4087-4094.

Miyawaki, A., Llopis, J., Heim, R., McCaffery, J.M., Adams, J.A., Ikura, M., and Tsien, R.Y. (1997). Fluorescent indicators for Ca2+ based on green fluorescent proteins and calmodulin. Nature *388*, 882-887.

Mukherjee, S., and Maxfield, F.R. (2000). Role of membrane organization and membrane domains in endocytic lipid trafficking. Traffic *1*, 203-211.

Neefjes, J. (1999). CIIV, MIIC and other compartments for MHC class II loading. Eur J Immunol *29*, 1421-1425.

Neefjes, J.J., Stollorz, V., Peters, P.J., Geuze, H.J., and Ploegh, H.L. (1990). The biosynthetic pathway of MHC class II but not class I molecules intersects the endocytic route. Cell *61*, 171-183.

Peters, P.J., Neefjes, J.J., Oorschot, V., Ploegh, H.L., and Geuze, H.J. (1991). Segregation of MHC class II molecules from MHC class I molecules in the Golgi complex for transport to lysosomal compartments. Nature *349*, 669-676.

Reits, E.A., and Neefjes, J.J. (2001). From fixed to FRAP: measuring protein mobility and activity in living cells. Nat Cell Biol *3*, E145-147.

Rocha, N., Kuijl, C., van der Kant, R., Janssen, L., Houben, D., Janssen, H., Zwart, W., and Neefjes, J. (2009). Cholesterol sensor ORP1L contacts the ER protein VAP to control Rab7-RILP-p150

Glued and late endosome positioning. J Cell Biol *185*, 1209-1225.

Roche, P.A., and Cresswell, P. (1990). Invariant chain association with HLA-DR molecules inhibits immunogenic peptide binding. Nature *345*, 615-618.

Rubinstein, E., Le Naour, F., Lagaudriere-Gesbert, C., Billard, M., Conjeaud, H., and Boucheix, C. (1996). CD9, CD63, CD81, and CD82 are components of a surface tetraspan network connected to HLA-DR and VLA integrins. Eur J Immunol *26*, 2657-2665.

Saffman, P.G., and Delbruck, M. (1975). Brownian motion in biological membranes. Proc Natl Acad Sci U S A *72*, 3111-3113.

Sanderson, F., Thomas, C., Neefjes, J., and Trowsdale, J. (1996). Association between HLA-DM and HLA-DR in vivo. Immunity *4*, 87-96.

Tarrant, J.M., Robb, L., van Spriel, A.B., and Wright, M.D. (2003). Tetraspanins: molecular organisers of the leukocyte surface. Trends Immunol *24*, 610-617.
Teis, D., Saksena, S., and Emr, S.D. (2009). SnapShot: the ESCRT machinery. Cell *137*, 182-182 e181.

Unternaehrer, J.J., Chow, A., Pypaert, M., Inaba, K., and Mellman, I. (2007). The tetraspanin CD9 mediates lateral association of MHC class II molecules on the dendritic cell surface. Proc Natl Acad Sci U S A *104*, 234-239.

van Rheenen, J., Langeslag, M., and Jalink, K. (2004). Correcting confocal acquisition to optimize imaging of fluorescence resonance energy transfer by sensitized emission. Biophys J *86*, 2517-2529.

Vennegoor, C., and Rumke, P. (1986). Circulating melanoma-associated antigen detected by monoclonal antibody NKI/C-3. Cancer Immunol Immunother *23*, 93-100.

Wubbolts, R., Leckie, R.S., Veenhuizen, P.T., Schwarzmann, G., Mobius, W., Hoernschemeyer, J., Slot, J.W., Geuze, H.J., and Stoorvogel, W. (2003). Proteomic and biochemical analyses of human B cell-derived exosomes. Potential implications for their function and multivesicular body formation. J Biol Chem *278*, 10963-10972.

Zwart, W., Griekspoor, A., Kuijl, C., Marsman, M., van Rheenen, J., Janssen, H., Calafat, J., van Ham, M., Janssen, L., van Lith, M.*, et al.* (2005). Spatial separation of HLA-DM/HLA-DR interactions within MIIC and phagosome-induced immune escape. Immunity *22*, 221-233.

Supplementary information

Table S1. Stable cell lines generated for this study

CELL LINE	CONSTRUCT 1	CONSTRUCT 2	CONSTRUCT 3	FIGURE
MelJuSo				1a, 1b, 1c
HEK293T				1b
HEK293T	HLA-DRA-IRES-HLA-DRB3-YFP	Ii p31		1a, 2b, 2c
HEK293T	HLA-DMA-IRES-HLA-DMB-CFP	HLA-DRA-IHRES-HLA-DRB3-YFP	Ii p31	1a, 2b, 2c
HEK293T	YFP-CD63			1b, 1c, 2a, 2b, 2c
HEK293T	YFP-CD82			1b, 1c, 2b, 2c
HEK293T	CFP-CD63	YFP-CD63		3, 4a
HEK293T	CFP-CD82	YFP-CD63		3, 4b
HEK293T	CFP-CD82	YFP-CD82		3, 4c
HEK293T	CFP-CD63	HLA-DRA-IHRES-HLA-DRB3-YFP	Ii p31	3, 5a
HEK293T	CFP-CD82	HLA-DRA-IHRES-HLA-DRB3-YFP	Ii p31	3, 5b
HEK293T	HLA-DMA-IRES-HLA-DMB-CFP	YFP-CD63		3, 6a
HEK293T	HLA-DMA-IRES-HLA-DMB-CFP	YFP-CD82		3, 6b

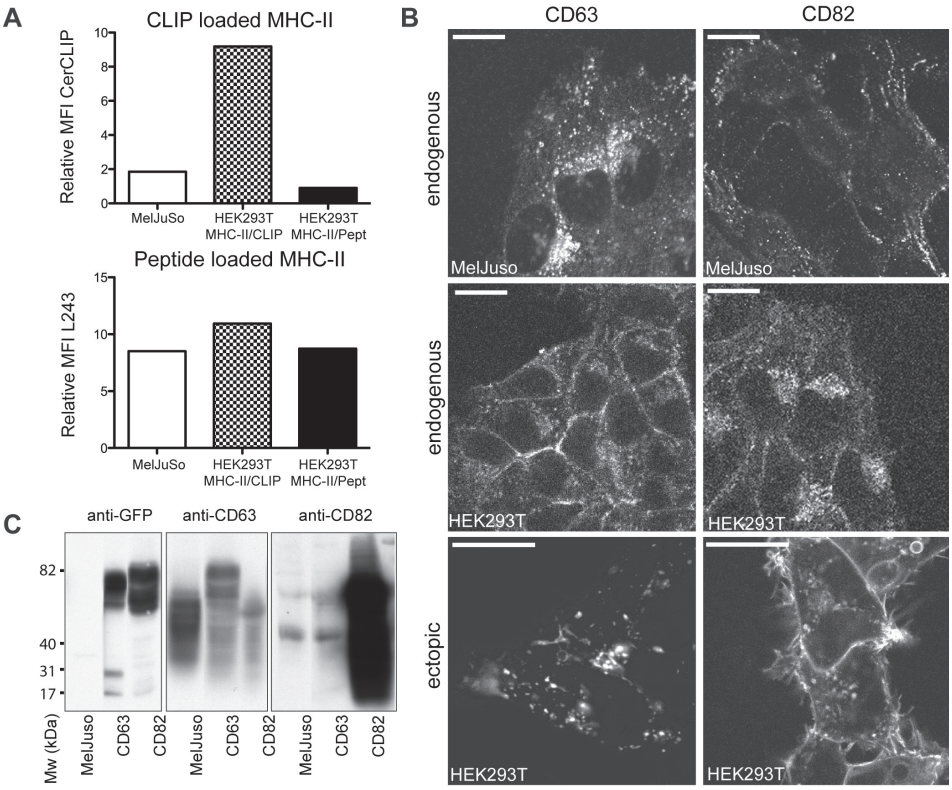

Fig. S1: Characterization of FRET pairs for functional MHC-II peptide loading and tetraspanin proteins in HEK293T cells. (A) Cell surface expression of MHC-II/CLIP (detected by CerCLIP antibody) and MHC-II/Peptide (detected by L243 antibody) on control MelJuSo cells and on HEK293T cells stably expressing MHC-II (HLA-DRα, HLA-DRβ-YFP, Ii) in the absence (HEK293T CLIP-MHC-II/CLIP) or presence (HEK293T MHC-II/Pept) of DM-CFP, as measured by flow-cytometry. Depicted is the Mean Fluorescence Intensity (MFI) relative to secondary antibody only. (B) Distribution of endogenous and YFP-tagged tetraspanins. MelJuSo and HEK293T cells were stained for endogenous CD63 or CD82 or the distribution of YFP-CD63 or YFP-CD82 was determined by CLSM. Bar: 20 nm. (C) Biochemical analysis of HEK293T cells expressing CFP- and YFP-CD63 (CD63) or CFP- and YFP-CD82 (CD82). Lysates of the transfectants CD63 and CD82 (and MelJuSo cells as control) were separated by SDS-PAGE and the Western Blot was incubated with anti-CD63, anti-CD82 or anti-GFP (recognizing YFP-tag and CFP-tag) antibodies, as indicated. The position of the molecular weight (Mw) standard is indicated.

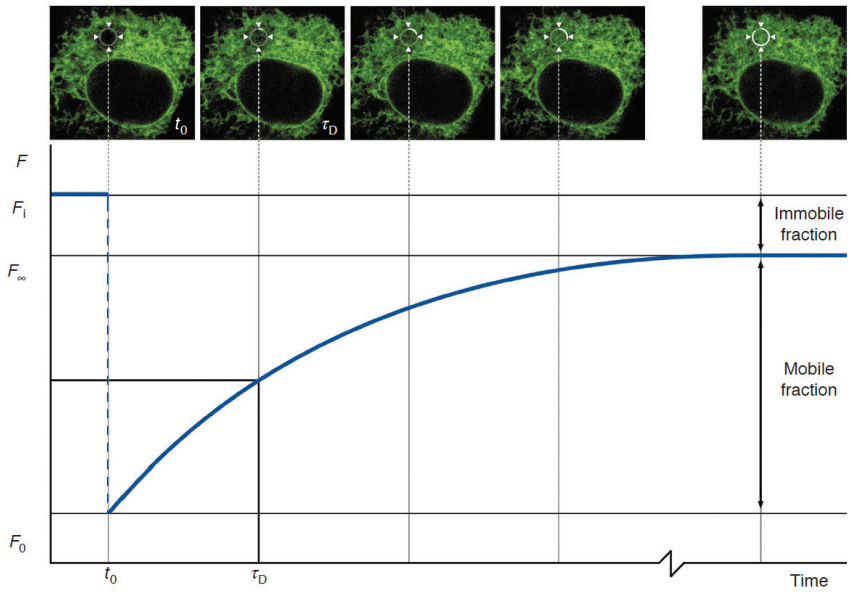

Fig. S2. Fluorescent intensity plotted against time in FRAP curve. When a region in the fluorescent area (here the endoplasmic reticulum) is bleached at time t_0 the fluorescence decreases from the initial fluorescence F_i to F_o. The fluorescence recovers over time by diffusion until it has fully recovered (F_∞). The characteristic diffusion time (τD) indicates the time at which half of the fluorescence has recovered. The mobile fraction can be calculated by comparing the fluorescence in the bleached region after full recovery (F_∞) with that before bleaching (F_i) and just after bleaching (F_o). The immobile fraction is the amount of fluorescence before bleaching minus the amount after full recovery (F_∞) (Reits & Neefjes, 2001).

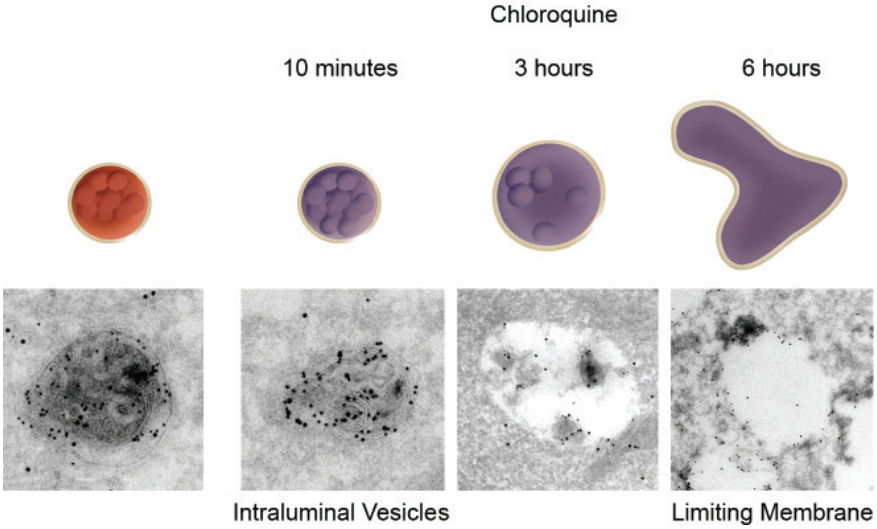

Fig. S3. Chloroquine causes neutralization and swelling of MVB. The MVB is an acidic compartment. Adding chloroquine to cells causes immediate (within ten minutes) neutralization of this compartment. When cells are incubated with chloroquine for three hours, MVBs reach a partially swollen state, still containing a few intraluminal vesicles in the MVB. After six hours of chloroquine incubation, MVBs are completely swollen, consisting of limiting membrane only. 10 nm gold particles represent DM and 15 nm gold particles represent HLA-DR (MHC class II).

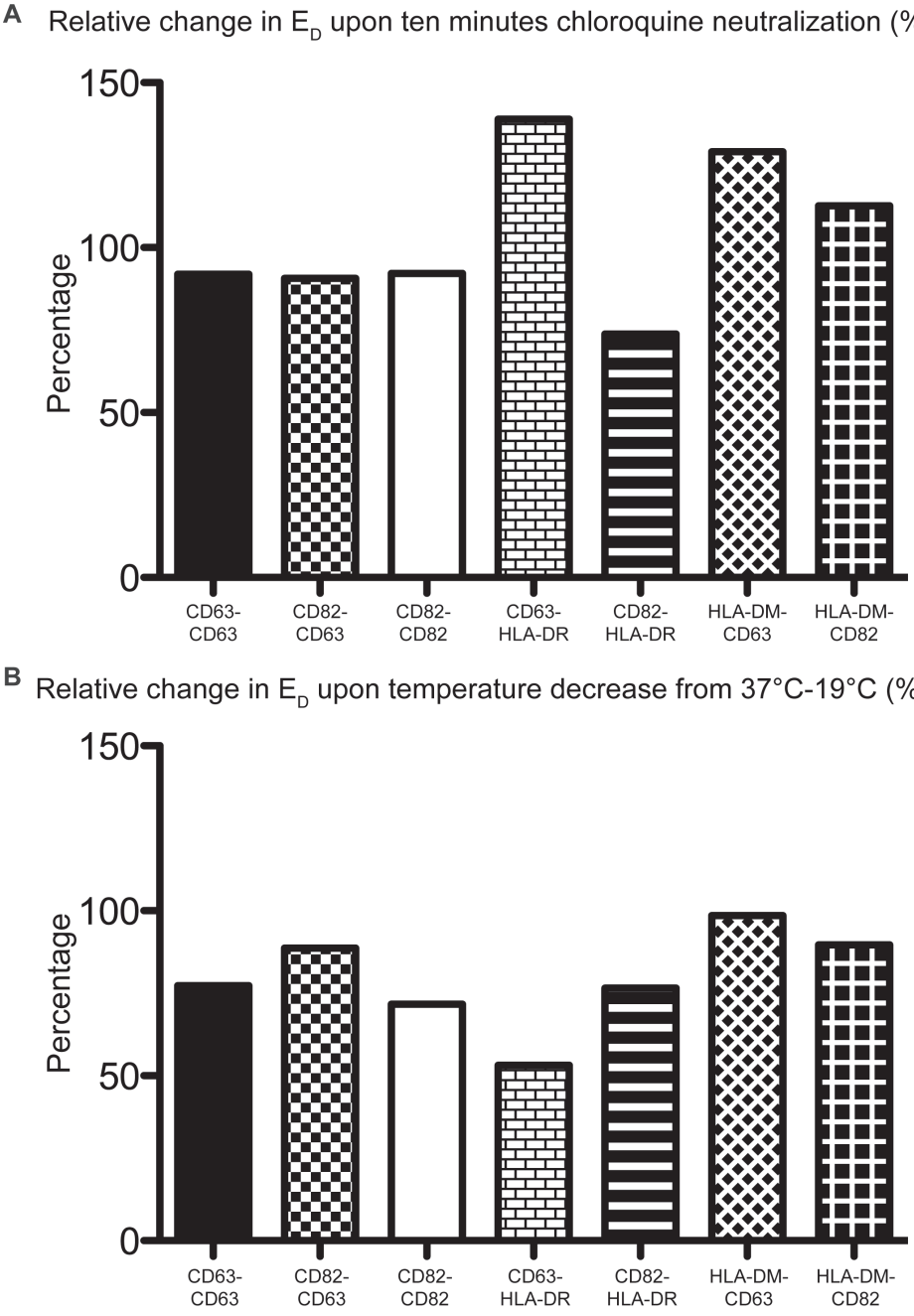

Fig. S4. Relative change of E_D upon neutralization Effects of chloroquine addition and temperature decrease on FRET E_D values. (A) Neutralization by incubation with chloroquine for ten minutes has various effects on E_D for the different pairs measured (control situation (19°C, without chloroquine) is set to 100%). (B) A change in temperature from 37°C to 19°C also decreases the E_D (37°C is set as 100%).